

Three-dimensional modelling of filamentary discharge using the SG Scheme coupling at time splitting method

Abstract. In this paper, we have developed a tri-dimensional numerical modelling of filamentary discharge, which enabled us to study the streamer discharge's propagation at high pressure, in a uniform electrical field. The transport equations and Poisson's equation formed self-consistent model. We use Scharfetter and Gummel schemes SG and SG0 coupling at time splitting method to resolve the transport equations system. The Poisson's equation is resolved by the tri-diagonal method coupled with the over-relaxation method to calculate the electrical field.

Streszczenie. W artykule opisano budowę modelu 3-D wyładowania włókienkowego, który posłużył do badań propagacji wyładowania wstęgowego przy wysokim ciśnieniu w jednorodnym polu elektrycznym. Model oparty jest na równaniach Poisson'a i transportu. W celu rozwiązania równań transportu, zastosowano metodę sprzężenia SG i SG0 Scharfetter'a i Gummela, natomiast do formuły Poisson'a zastosowano metodę trójkątną, w połączeniu z metodą SOR (ang. Successive Over-Relaxation method). (Trójwymiarowe modelowanie wyładowania włókienkowego, z wykorzystaniem metody SG sprzężenia przy podziale czasu).

Keywords: 3D Fluid Model, streamer discharge, SG Scheme, Time Splitting Method.

Słowa kluczowe: model cieczy w 3-D, wyładowanie wstęgowe, struktura SG, metoda podziału czasu.

Introduction

The electric discharges at atmospheric pressure and in particular the streamer discharge are usually used to produce plasmas usable for many industrial applications [1] [2]. A considerable amount of theoretical, numerical and experimental effort has been devoted to understand the development of an electron avalanche, its transition into streamers and the streamer fronts propagation [3]. The numerical modeling of the streamer discharge can provide an invaluable help in the field of plasmas. Many difficulties arise with the solution of the continuity equations, due to the very steep shock-like gradients that appear in such calculations, and, as a result, a very accurate numerical technique is required to capture their development. The filamentary discharges modeling in two dimensions spreads only since one ten years when a tri-dimensional modelling stills in an embryonic state and is developing slowly [4][5].

In this work, we developed a numerical code able to model a streamer discharge in three dimensions in a nitrogen gas at high pressure. The transport equations are solved by Scharfetter and Gummel SG, SG0 schemes. The validity test of our 3D code is carried out by comparing our results with the literature.

Hydrodynamic Model

The adopted model to determine the streamer dynamics is the order 1 model fluid. In which we limit ourselves at the two firsts momentums of the Boltzmann equation for the charged species. For that, we admit, on the one hand, the assumption of the local field, and on the other hand, the negligence of the higher order density gradient terms to close the transport equations system. In this hydrodynamic model, the transport equations of the charged particles are coupling with the Poisson's equation.

The equations which we used are the same ones as those introduced by Dhali and Williams [6] [7]:

The transport equations derived from first two moments of the Boltzmann's equation are written only for electrons and positive ions. These charged species constitute the active species in our electric discharge model.

The continuous equations describing the spatiotemporal variation (\vec{r}, t) of the charged spaces densities $n(\vec{r}, t)$ in this discharge take the forms [3, 8]:

$$(1) \quad \frac{\partial n(\vec{r}, t)}{\partial t} + \frac{\partial \Phi(\vec{r}, t)}{\partial \vec{r}} = S(\vec{r}, t)$$

where $\vec{r}(x, y, z)$ is the position vector.

The terms sources $S(\vec{r}, t)$ used by [6][7][9] are given by

(2):

$$S_e = S_p = \alpha \mu_e n_e E$$

(2)

$$\alpha = 5.7 P \exp(-260 P/E)$$

In the model, the momentum conservation equation is replaced by drift-diffusion approximation; hence, the transport equation is represented by two separate terms, i.e., drift and diffusion terms. The fluxes of the charged spaces densities are given by:

$$(3) \quad \Phi(\vec{r}, t) = n(\vec{r}, t)W(\vec{r}, t) - D(\vec{r}, t) \frac{\partial n(\vec{r}, t)}{\partial \vec{r}}$$

The Poisson's equation (4) is resolved for determination the electric field and the potential in the electrical discharge.

$$(4) \quad \frac{\partial E}{\partial \vec{r}} = \frac{e}{\epsilon_0} \rho(\vec{r}, t)$$

$\rho(\vec{r}, t)$ represents the net charge density.

Initials and boundaries Conditions

The numerical resolution of the transport equations in our 3D fluid model requires beforehand introduction of the boundary conditions and the initial conditions. According to specialized literature the numerical solution of the partial differential equations depends essentially of the conditions nature and the integration steps. In this paper, we used essentially the Neumann's conditions on the symmetric axis for electronic and ionic densities, and also for the electrical potential (see Fig. 1).

For the gradient particle densities at the right electrode:

the gradient ion density $\frac{\partial n_p}{\partial x} = 0$, and for the electron

density $\frac{\partial n_e}{\partial x} = 0$.

The Dirichelet boundaries conditions for the electric potential at electrodes are 26 KV at the powered electrode (anode) and 0 V at the grounded electrode (cathode).

At the left electrode: the gradient ion density $\frac{\partial n_p}{\partial x} = 0$,

and for the electron density $\frac{\partial n_e}{\partial x} = 0$.

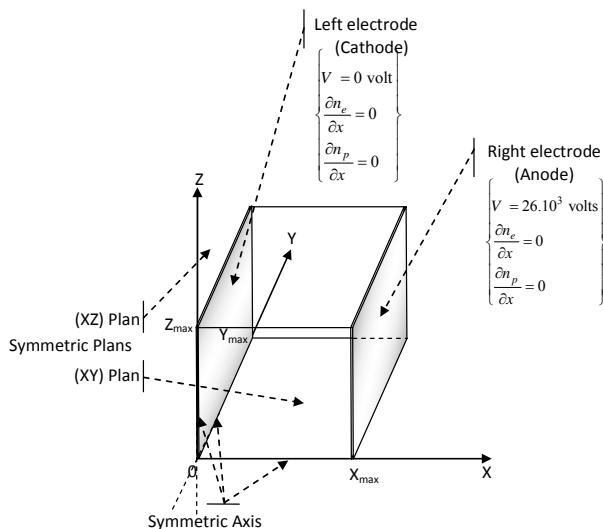


Fig.1. Schematic representation of the used boundaries conditions

Numerical model and SG-time splitting method

The multidimensional resolution of the continuity equations for the particles charged is carried out by using the method of the fractional steps [4][7][10]. This method consists in replacing the three-dimensional equations of transport (1) by a succession of the mono-dimensional equations in the object to reduce considerably the calculation time in each direction of space as the following expressions:

$$(5) \quad \frac{\partial n}{\partial t} + \frac{\partial \Phi}{\partial x} = 0$$

$$(6) \quad \frac{\partial n}{\partial t} + \frac{\partial \Phi}{\partial y} = 0$$

$$(7) \quad \frac{\partial n}{\partial t} + \frac{\partial \Phi}{\partial z} = 0$$

$$(8) \quad \frac{\partial n}{\partial t} = S$$

The opportunity of this new strategy of solution resides in the stability and the fast convergence toward the searched solution. We also mention the simplicity of the programming the equations system and an important gain in the CPU time [11].

The adapted scheme to solve the equations 5, 6 and 7 is the Scharfetter and Gummel scheme. In this paper, we combine between the SG and the SG0 scheme whose are presented by Kulikovskiy [12].

The calculated flux by SG scheme is given by the following expression:

$$(9) \quad \Phi_{i+1/2} = \frac{D_{i+1/2}}{h_i I_0} (n_i - e^{\alpha_i} n_{i+1})$$

$$\text{With: } h_i = x_{i+1} - x_i, \alpha_i = \frac{\mu h_i E_i}{D_{i+1/2}} \text{ and } I_0 = \frac{e^{\alpha_i} - 1}{\alpha_i}$$

$$\text{When: } h_i \ll \frac{2D_{i+1/2}}{\mu |\Delta E_i|},$$

The calculated flux expression is given by the improved scheme of order 0; SG0 as follows:

$$(10) \quad \Phi_{i+1/2} = \frac{D_{i+1/2}}{h_i I_0} (n_G - e^{\alpha_i} n_D)$$

$$\text{with: } h_v = \sqrt{2 \varepsilon D_{i+1/2} h_i / \mu |E_{i+1} - E_i|},$$

$$\alpha_v = \frac{\mu h_v E_i}{D_{i+1/2}} \text{ and } I_0 = \frac{e^{\alpha_v} - 1}{\alpha_v}$$

The densities n_G and n_D at the virtual nodes are given by the following expressions:

$$(11) \quad n_G = (n_i + I) e^{a(x_G - x_i)} - I$$

$$(12) \quad n_D = (n_i + I) e^{a(x_D - x_i)} - I$$

$$\text{With: } a = \frac{1}{h_i} \log \left(\frac{n_{i+1} + I}{n_i + I} \right), \text{ and,}$$

$$x_G = (x_i + x_{i+1} - h_v) / 2, \quad x_D = (x_i + x_{i+1} + h_v) / 2$$

Results and Interpretations

The 3D hydrodynamic model, that we described, makes possible to study macroscopically this type of electrical discharge. For that, we chose the discharge conditions similar to those of [6]: The pressure P of nitrogen gas is as 760 Torr, its temperature is 300°K, the distance inter electrodes is 0.5 cm and the potential applied to the anode is 26 KV, which corresponds to an electric field of 52 KV/cm.

Table.1. Transport parameters used in the present simulation [6][7]

Transport parameters	Values
N	$2.83 \cdot 10^{16} \text{ (cm}^{-3}\text{)}$
$D_{e,x}$	$1800 \text{ (cm}^2\text{s}^{-1}\text{)}$
$D_{e,y}$	$2190 \text{ (cm}^2\text{s}^{-1}\text{)}$
$D_{e,z}$	$2190 \text{ (cm}^2\text{s}^{-1}\text{)}$
$D_{p,x} = D_{p,y} = D_{p,z}$	$10 \text{ (cm}^2\text{s}^{-1}\text{)}$
μ_e	$2.9 \cdot 10^5 / P \text{ (cm}^2\text{V}^{-1}\text{s}^{-1}\text{)}$
μ_p	$2.6 \cdot 10^3 / P \text{ (cm}^2\text{V}^{-1}\text{s}^{-1}\text{)}$
X_{\max}	0.5 (cm)
Y_{\max}	0.5 (cm)
Z_{\max}	0.5 (cm)

Throughout this work, we use an initial gaussian profile, placed on the symmetry axis

$$n(x, y, z) = n_0 \cdot \exp \left[-\left(\frac{x}{\sigma_x} \right)^2 - \left(\frac{y}{\sigma_y} \right)^2 - \left(\frac{z}{\sigma_z} \right)^2 \right] + 10^8$$

with,

$$n_0 = 10^{14} \text{ cm}^{-3}, \sigma_x = 0.027 \text{ cm}, \sigma_y = 0.021 \text{ cm}, \sigma_z = 0.021 \text{ cm}$$

To validate our developed code, we compared our results 3D represented along the symmetric axis of propagation in 1D with those of Dhali and Williams [6] concerning the negative streamer's propagation.

Fig. 2 and 3 show our results and those obtained by Dhali and Williams of the electronic densities profiles and the electric field at different instants: 1.0, 2.0, 2.5 and 3.0 ns.

The comparisons carried out above show that the results resulting from our model 3D are physically realistic and close to those obtained by Dhali and Williams [6]. The orders of magnitude being almost the same ones with some light differences. Most notable is the propagation velocity of our streamer, which is lower than that of Dhali and Williams for times 2.5 and 3.0 ns. The calculated electric field is always lower than that obtained by Dhali and Williams during every moment except for that of 3.0 ns.

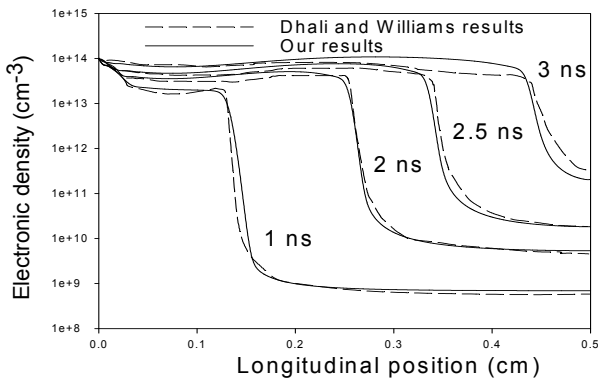


Fig. 2: electron density propagation on symmetrical axis at different instants

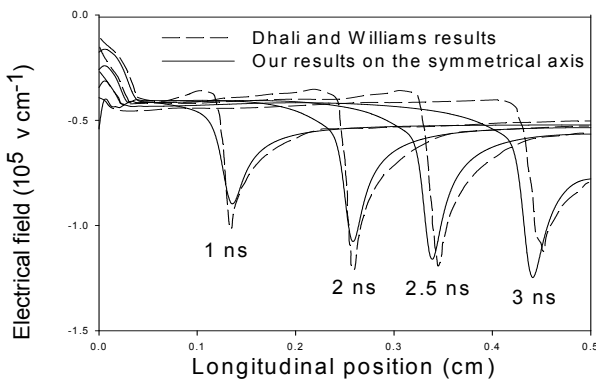


Fig. 3: longitudinal electric field evolution on symmetrical axis at different instants.

Nevertheless, we can justify these slight differences by the use of a numerical model 3D which is different from the model 2D used by Dhali and Williams. The use of different parameters in our model can change the characteristics of the streamer considerably, such as: the numerical method used to resolve the numerical model, the source term, the number of points of discretization and the temporal evolution step.

According to the above validation test, we can say that our 3D code is able to reproduce the physical and electric mechanisms of the negative streamer propagation. We analyze the various phases of propagation of the filament discharge and the principal mechanisms which control it.

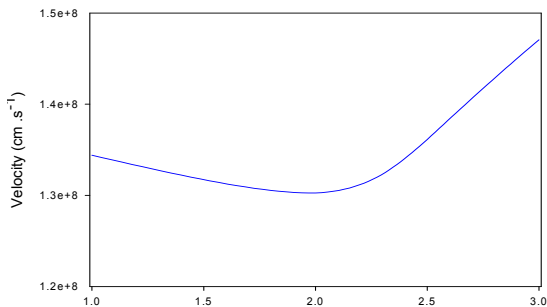


Fig. 4: streamer propagation velocity variations

Fig. 4 represents the velocity variation according to time. This calculated velocity, starting from our code results, is deduced from the head discharge advance according to the propagation axis. We notice that the streamer velocity decrease slightly until a minimum for a time lower than 2.0

ns. This propagation phase is posterior with an important space charge creation in the initial moment at the cathode.

From this moment, the electronic density and the electric field grow in a regular way. The initiating electrons number increases and becomes increasingly important. It leads to a real increase in the ionization effectiveness. The streamer head propagation velocity grows in a monotonous way.

For the higher times than 1.0 ns, the final structure of the filament discharge appears. The variation of the electronic density on the streamer head is extremely fast as well as the electric field variation.

Fig. 5 to Fig. 8 represent the tri-dimensional electronic density propagation and the tri-dimensional longitudinal, transversal and tangential fields' evolution, at different instants 1.0, 2.0, 2.5 and 3.0 ns respectively.

Fig. 5 shows the longitudinal propagation of the streamer discharge and its transversal and tangential extensions.

In consequence of the ionization and displacement of the electrons joint influence towards the anode, the longitudinal, transversal and tangential components of the electric field become very important on the streamer head. They involve a permanent widening of the electronic cloud according to the time (see Fig. 6, 7, 8).

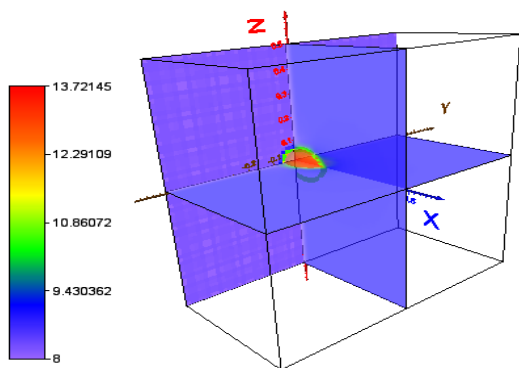
On the Fig. 7 and Fig.8, we can distinguish the streamer containment in inter electrodes space due to the presence of the transversal and tangential fields which will allow its displacement along the longitudinal propagation axis (axis of symmetry in our case).

All the presented results figures show the existence of two distinct areas inside the streamer. First is consisted of head and body filament discharge. This area constitutes the dynamic zone of the discharge because it makes it possible to create the conditions of ionization necessary to the propagation of the streamer. The second area ensures the permanent flow of the charged spaces collected at the streamer head.

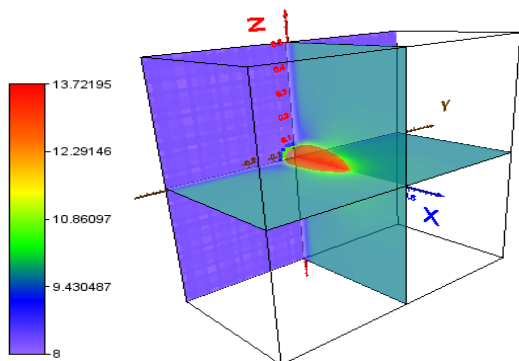
The streamer head propagation, where the electric field is maximal, is directly under control of the ionization mechanisms inside gas when the filamentary discharge ray depends on it slightly.

Conclusion

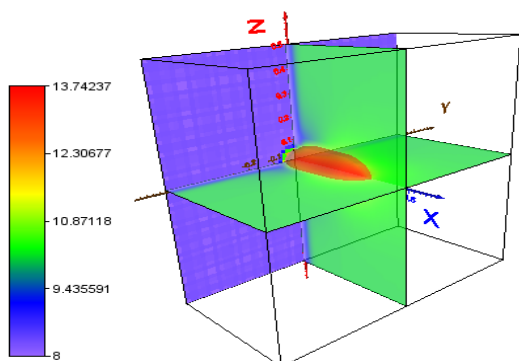
In this paper, we have developed a tri-dimensional numerical model of negative streamer discharge. The fully three-dimensional calculations of streamer dynamics will provide a suitable test case for streamer models as they predict easily observable comportment [10]. This resolution of the transport equations coupled with the Poisson's equation enabled us to study the dynamics of the particles charged in the case of a negative streamer with high pressure, for a better comprehension of the evolution and the propagation of filamentary discharge in situations of strong variations of density and electric field. One run of our model took approximately ten hours using a personal computer Intel Dual Core 1.80 GHz with RAM capacity of 1 Go. The main advantages of our model include the fully tri-dimensional approach; low time with low hardware configuration requirements.



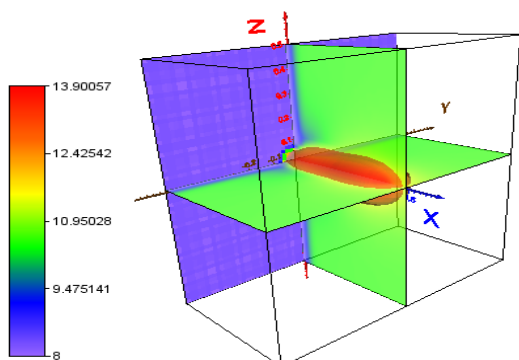
instant: 1.0 ns



instant: 2.0 ns

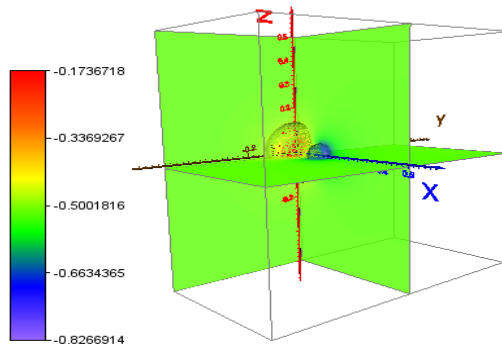


instant: 2.5 ns

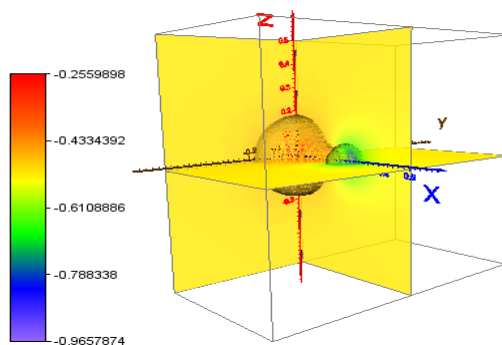


instant: 3.0 ns

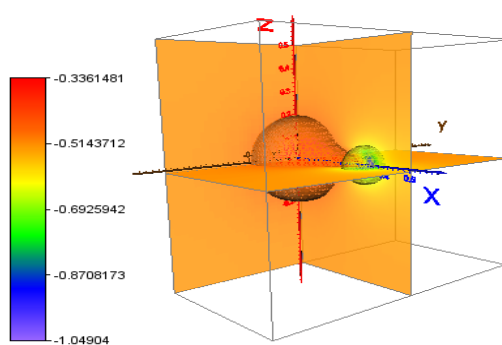
Fig. 5: 3D electron density propagation at different instants ($\log_{10}(n_e)\text{cm}^{-3}$).



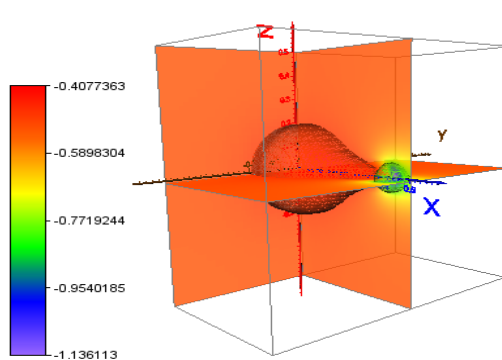
instant: 1.0 ns



instant: 2.0 ns

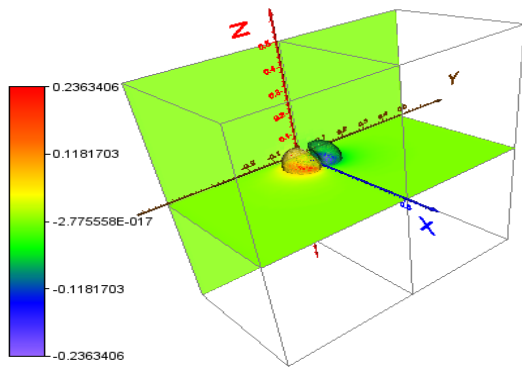


instant: 2.5 ns

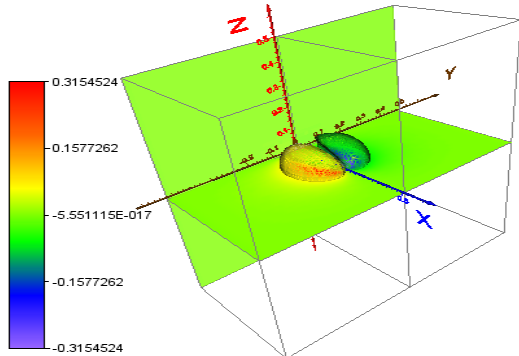


instant: 3.0 ns

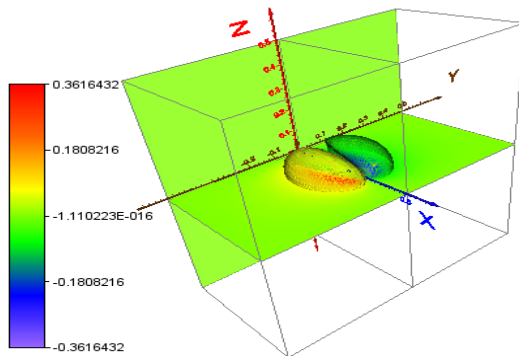
Fig. 6: 3D longitudinal electric field evolution at different instants ($10^5 \text{ V}\cdot\text{cm}^{-1}$).



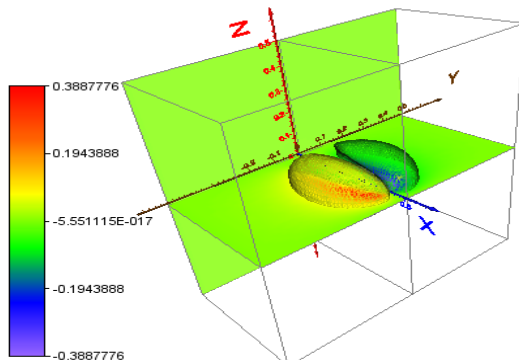
instant: 1.0 ns



instant: 2.0 ns

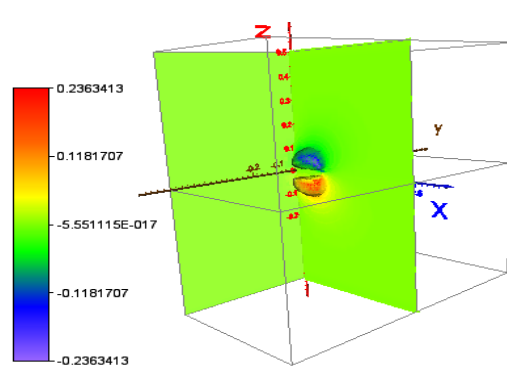


instant: 2.5 ns

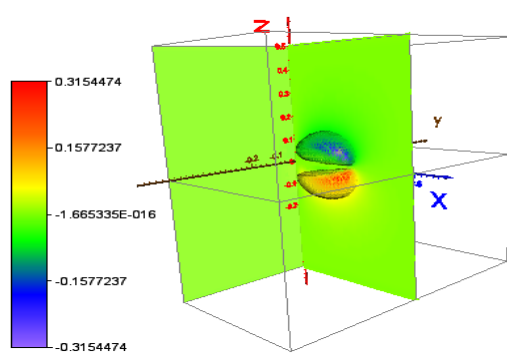


instant: 3.0 ns

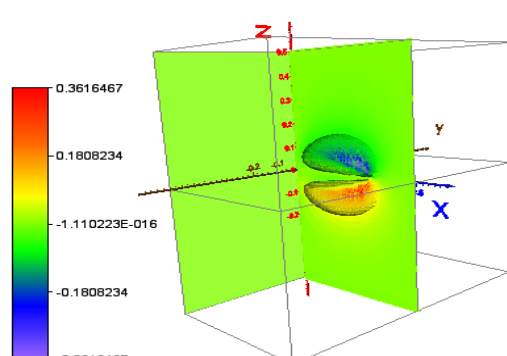
Fig. 7: 3D transversal electric field evolution at different instants ($10^5 \text{ V}\cdot\text{cm}^{-1}$).



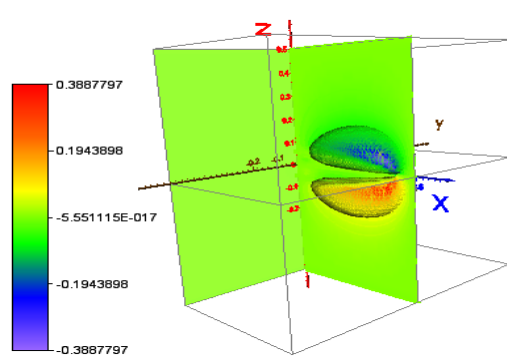
instant: 1.0 ns



instant: 2.0 ns



instant: 2.5 ns



instant: 3.0 ns

Fig. 8: 3D tangential electric field evolution at different instants ($10^5 \text{ V}\cdot\text{cm}^{-1}$).

Nomenclature

Index e and p used for electron and positive ion respectively

n	Number density
Φ	Charged species flux
S	Term source
V	Electric potential
E	Electric field
μ	Mobility of charged species
D	Diffusion coefficient of charged species
α	Ionisation coefficient
W	Drift velocity
P	Pressure
N	Density of the neutral gas
e	Elementary charge
ϵ_0	Permittivity of free space
X_{\max}	Longitudinal inter-electrode gap
Y_{\max}	Transversal inter-electrode gap
Z_{\max}	Tangential inter-electrode gap
Δx	Longitudinal spatial step
Δy	Transversal spatial step
Δz	Tangential spatial step
Δt	Temporal step

REFERENCES

- [1] Akiyama H., Streamer discharges in liquids and their applications, *Dielectrics and Electrical Insulation, IEEE Transactions*, 7(2000)No. 5, 646-653
- [2] Ishikawa A., Himeno H., Saito T., Sugai T., Minamitani Y., The sterilization of underwater bacteria by pulsed streamer discharge generated in air spraying water droplets, *Plasma Science, 2010 Abstracts IEEE International Conference*
- [3] Georghiou G. E., Papadakis A. P., Morrow R., Metaxas A. C., Numerical modelling of atmospheric pressure gas discharges leading to plasma production, *J. Phys. D: Appl. Phys.*, 38(2005), No. 20, R303-R328
- [4] Bessieres D. Modélisation des décharges filamenteuses, *Thèse de Doctorat. Université de Pau et des pays de l'Audour, France*, (2006)
- [5] Pancheshnyi S., Role of electronegative gas admixtures in streamer start, propagation and branching phenomena, *Plasma Sources Sci. Technol.*, 14(2005), 645-653
- [6] Dhali S. K., Williams P. F., Two-dimensional studies of streamers in gases, *J. Appl. Phys.*, 62(1987), No. 12, 4696-4708
- [7] Potin J. Modélisation numérique d'une décharge filamentaire contrôlée par barrière diélectrique dans l'azote à la pression atmosphérique. *Thèse de Doctorat, Université Paul Sabatier de Toulouse, France*, (2001).
- [8] Montijn C., Ebert U., Hundsdorfer W., Adaptive grid simulations of negative streamers in nitrogen in under- and overvoltage gaps, *XXVIIth ICPIG, Eindhoven, the Netherlands*, 18-22 July(2005), 17-21
- [9] Luque A., Ebert U., Hundsdorfer W., Interaction of streamer discharges in air and other oxygen-nitrogen mixtures, *Phys. Rev. Lett.*, 101(2008), No. 7, 075005
- [10] Hundsdorfer W., Portero L., A note on iterated splitting schemes, *Journal of Computational and Applied Mathematics*, 201(2007), 146-152
- [11] Kraloua B., Hennad A., Bidimensional modelling non-equilibrium fluid model of glow discharge at low pressure, *International Review of Electrical Engineering*, 5(2010), No. 6, 2653-2656
- [12] Kulikovskiy A. A., Positive streamer between parallel plate electrodes in atmospheric pressure air, *J. Phys. D: Appl. Phys.*, 30(1997), No. 3, 441-450

Authors

Noredine Benaired was born in Relizane, Algeria, on January, 15, 1977. His scientific interests include the theoretical study and modeling of physical processes in gas discharge plasma. E-mails: nbenaired@yahoo.fr

Ali Hennad was born in Oran, Algeria, on January, 27, 1964. He received the PH.D degree with a thesis on the kinetics of ions in molecular gases to determine ion basic data in air from Monte Carlo simulation, University Paul Sabatier of Toulouse, France in 1996. He is currently a Professor at University of Sciences and Technology of Oran, Algeria. His field of expertise is more particularly the modeling of the electric and hydrodynamic behaviors of the plasmas generated in low and high pressure. He has also a good expertise on the numerical analysis of the nonlinear and strongly coupled elliptic transport equations, and the swarm parameters determination of the charged particles in non equilibrium reactive plasma. He is the author of various international publications, a lot of them in collaboration with the LAPLACE Laboratory, Toulouse, France. E-mails: ali_hennad@yahoo.fr